Paper: ASAT-15-135-MO

15th International Conference on
AEROSPACE SCIENCES & AVIATION TECHNOLOGY,
ASAT - 15 – May 28 - 30, 2013, Email: asat@mtc.edu.eg ,
Military Technical College, Kobry Elkobbah, Cairo, Egypt,
Tel: +(202) 24025292 –24036138, Fax: +(202) 22621908

A Complete Control System Design for a Tactical Missile Using Model Predictive Control

{M. S. Mohamed[*], A. M. Bayoumy[†], A. A. El-Ramlawy[‡] }[§], and G. A. El-Sheikh[**]

Abstract: During the last decade, a significant research effort has been contributed in the area of non-linear missile autopilot design. But in some kinds of missiles, the classical controllers are still effective and very robust provided that the controller can adapt itself with missile varying parameters and this makes the control implementation and algorithm complicated as it changes with flight conditions. In this paper roll and lateral autopilots are designed for short range surface-to-surface aerodynamically controlled missile using model predictive control with fixed algorithm along the whole flight time. From linearization of missile non-linear model, transfer functions are determined and then discretized. The controllers are designed using Model-based predictive control techniques with fixed algorithm and insure that they can achieve full flight envelope control capability. Finally, the designed controllers are conducted into 6DOF simulation (individually and all-together) which is carried out using the Matlab-Simulink software.

Keywords: Missile autopilot design, roll control, normal acceleration control, lateral acceleration control, model-based predictive control.

Nomenclature

a_n	Normal acceleration	u	Input signal
a_{nc}	Commanded normal acceleration	u_0	Undisturbed longitudinal velocity
K	Sample number	u_η	Control signal
L_p	Rolling moment due to roll rate	V_{xf}, V_{yf}, V_{zf}	Velocity of body c.g. w.r.t. Earth axis
L_ξ	Rolling moment due to aileron angle	X_u	Axial force due to longitudinal velocity
l_p	Position of accelerometer in front of c.g.	x_f, y_f, z_f	Position of body c.g. w.r.t. Earth axis
M. O.	Maximum percentage overshoot	Y_r	Side force due to yaw rate
Ma	Mach number	Y_v	Side force due to side velocity
M_q	Pitching moment due to pitch rate	Y_ζ	Side force due to rudder angle
M_w	Pitching moment due to vertical velocity	y	Output vector
M_α	Pitching moment due to angle of attack	Z_q	Normal force due to pitch rate
M_η	Pitching moment due to elevator angle	Z_w	Normal force due to vertical velocity
N_2	Prediction horizon	Z_α	Normal force due to angle of attack
N_r	Yawing moment due to yaw rate	Z_η	Normal force due to elevator angle

[*] m_saad43@hotmail.com
[†] ambayoumy@gmail.com
[‡] abaset92@yahoo.com
[§] Egyptian Armed Forces, Egypt.
[**] Prof. Pyramids Higher Institute for Engineering and Technology, gaelsheikh@gmail.com

N_u	Control horizon	α	Angle of attack
N_v	Yawing moment due to side velocity	β	Side slip angle
N_ζ	Yawing moment due to rudder angle	ζ	Rudder angle
p, q, r	Roll, pitch and yaw rates	η	Elevator angle
Q	Dynamic pressure	θ	Pitch angle
T_s	Sampling time	ξ	Aileron angle
T	Time	φ	Roll angle
t_r	Rise time	ψ	Yaw angle
t_s	Settling time	ω_n	Short period mode natural frequency
u, v, w	Velocity component in body axes		

1. Introduction

A navigation system is one that automatically determines the position of the vehicle with respect to some reference frame, for example, the earth. If the vehicle is off course, it is up to the operator to make the necessary correction. A guidance system, on the other hand, automatically makes the necessary correction to keep the vehicle on course by sending the proper signal to the control system or autopilot. The guidance system then performs all the functions of a navigation system plus generating the required correction signal to be sent to the control system [1]. Figure 1 shows the block diagram of guidance, navigation and control system. The function of the autopilot subsystem can be defined as follows:

- Provide the required missile normal and lateral acceleration response characteristics.
- Stabilize or damp the airframe roll angle.
- Reduce the missile performance sensitivity to disturbance inputs over the missile's flight envelope.

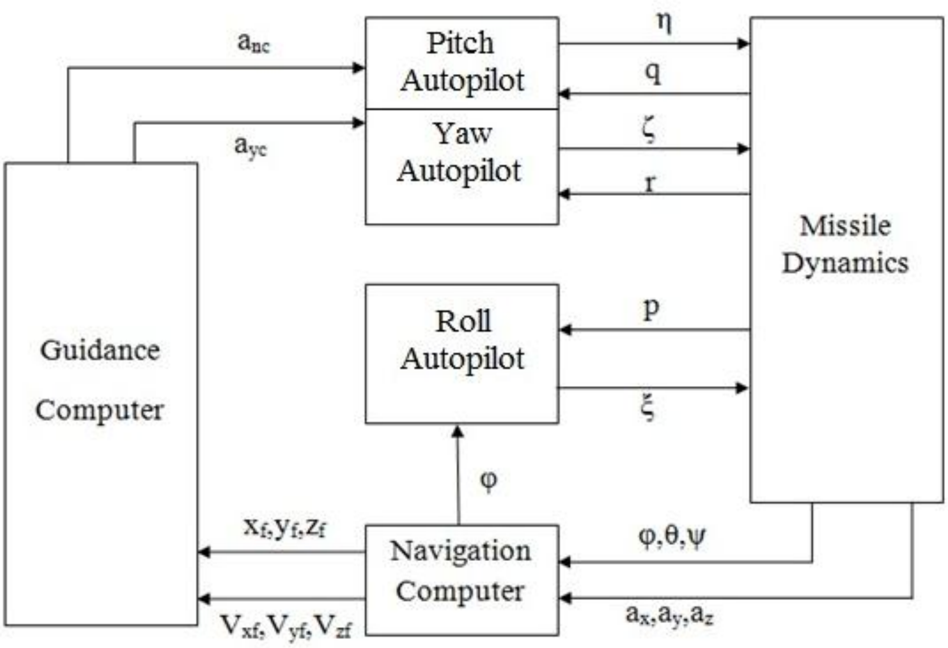

Fig. 1 Block diagram of guidance, navigation and control

Roll autopilot receives the roll angle (φ) signal from navigation computer and roll rate (p) from rate-gyro unit to send the desired aileron angle to the aerodynamic fins to eliminate the missile roll angle.

Lateral autopilots receive the commanded lateral acceleration signals from guidance computer (anc, ayc) and pitch and yaw rates (q, r) from the rate-gyro unit to send the desired elevator and rudder angles (η, ζ) to the aerodynamic fins which control the attitude of the missile. In this paper, roll angle, normal and lateral acceleration autopilots for a surface-to-surface missile are designed using predictive control techniques. The predictive controller will utilize single model to control both normal and lateral acceleration and roll angle along trajectory. Simulation is created for the whole system as a closed-loop system to verify the performance of the designed systems.

2. Missile Model

Equations of motion from [1] and [2], aerodynamic coefficients are calculated from [3] and as represented in [4].

Linearization of Missile Model

The linear equations needed for control system design will be derived using the small perturbation method from the nonlinear model. In [5], a complete linearization for force and moment equations in the state model is presented for design of model-predictive controllers. The six equations of motion can be written as:

$$\begin{bmatrix} \Delta\dot{u} \\ \Delta\dot{v} \\ \Delta\dot{w} \\ \Delta\dot{p} \\ \Delta\dot{q} \\ \Delta\dot{r} \end{bmatrix} = \begin{bmatrix} X_u & 0 & 0 & 0 & 0 & 0 \\ 0 & Y_v & 0 & 0 & 0 & (Y_r - u_0) \\ 0 & 0 & Z_w & 0 & (u_0 + Z_q) & 0 \\ 0 & 0 & 0 & L_p & 0 & 0 \\ 0 & 0 & M_w & 0 & M_q & 0 \\ 0 & N_v & 0 & 0 & 0 & N_r \end{bmatrix} \begin{bmatrix} u \\ v \\ w \\ p \\ q \\ r \end{bmatrix} + \begin{bmatrix} 0 & 0 & 0 \\ 0 & 0 & Y_\zeta \\ 0 & Z_\eta & 0 \\ L_\xi & 0 & 0 \\ 0 & M_\eta & 0 \\ 0 & 0 & N_\zeta \end{bmatrix} \begin{bmatrix} \xi \\ \eta \\ \zeta \end{bmatrix} \quad (1)$$

3. Design Considerations

Introduction

Model Based Predictive Control (MPC) is a control methodology which uses on-line process model for calculating predictions of the future plant output and for optimizing future control actions. In fact MPC is not a single specific control strategy but rather a family of control methods which have been developed with certain ideas in common. According to Fig. 2, the future outputs for a determined horizon N, called the prediction horizon, are predicted at each instant t using the process model as shown in Eqn (2).

$$y(k+i\,|\,k) = C_d A_d^{\,i} X(k) + \sum_{j=0}^{i-1} C_d \left(A_d^{\,j} B_d u(k-1) + \left(\sum_{h=0}^{i-j-1} A_d^{\,h} B_d \right) \Delta u(k+j) \right) \quad (2)$$

Then the set of future control signals is calculated by optimizing a determined criterion in order to keep the process as close as possible to the reference trajectory $a_{nc}(t + k)$. Finally, The control signal u(t | t) is sent to the process whilst the next control signals calculated are rejected, because at the next sampling instant y(t + 1) is already known and repeating with this new value and all the sequences are brought up to date.

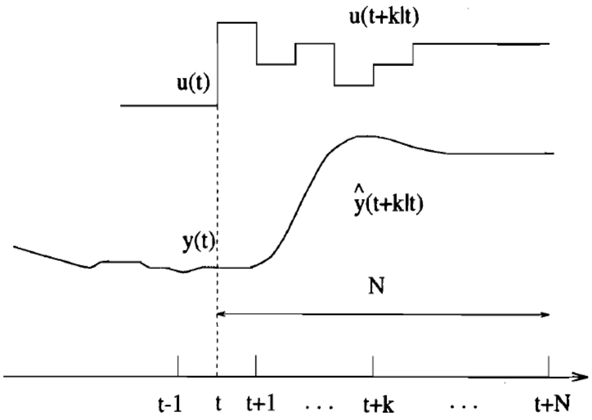

Fig. 2 MPC strategy

MPC is a digital control strategy. It uses a discrete linear model of the plant as a predictor of its future behavior. The control sequence applied to the plant is the optimum calculated sequence that provides minimum value for the objective function J as shown in Eqn (3).

$$J=\min\left\{\sum_{i=0}^{p-1}\left(\begin{array}{l}\displaystyle\sum_{j=N_1}^{N_2}\left|w_{i+1,j}^{y}\left(y_j(k+i+1|k)-r_j(k+i+1)\right)\right|^2+\sum_{j=1}^{N_u}\left|w_{i,j}^{\Delta u}\Delta u_j(k+i|k)\right|^2\\ \displaystyle+\sum_{j=1}^{N_u}\left|w_{i,j}^{u}(u_j(k+i|k)-\bar{u}_j)\right|^2\end{array}\right)\right\} \tag{3}$$

$w_{i,j}^{u}$, $w_{i,j}^{\Delta u}$, $w_{i,j}^{y}$ are nonnegative weights for the input, input rate and output respectively. Normally, the objective is chosen to be a combination of output tracking error and control energy. This optimization could be constrained either by input or output constraints [6].

Design Goals and Requirements

The task of the control system is to produce the necessary rolling moment, normal and lateral forces and maneuver the missile (change the direction of the missile velocity vector) quickly and efficiently as a result of guidance signals [1]. Considering first-order lag actuator of transfer function (60/(s+60)) and unity gain free-gyro, rate-gyro and accelerometer, the state-space of roll, pitch and yaw autopilots yields:

$$\begin{gathered}\begin{bmatrix}\dot{\phi}\\ \dot{p}\\ \dot{\xi}\end{bmatrix}=\begin{bmatrix}0 & 1 & 0\\ 0 & L_p & L_\xi\\ 0 & 0 & -60\end{bmatrix}\begin{bmatrix}\phi\\ p\\ \xi\end{bmatrix}+\begin{bmatrix}0\\ 0\\ 60\end{bmatrix}u_\xi\\ \begin{bmatrix}\phi\\ p\end{bmatrix}=\begin{bmatrix}1 & 0 & 0\\ 0 & 1 & 0\end{bmatrix}\begin{bmatrix}\phi\\ p\\ \xi\end{bmatrix}\end{gathered} \tag{4}$$

$$\begin{gathered}\begin{bmatrix}\dot{\alpha}\\ \dot{q}\\ \dot{\eta}\end{bmatrix}=\begin{bmatrix}Z_w & 1+\dfrac{Z_q}{u_0} & \dfrac{Z_\eta}{u_0}\\ M_\alpha & M_q & M_\eta\\ 0 & 0 & -60\end{bmatrix}\begin{bmatrix}\alpha\\ q\\ \eta\end{bmatrix}+\begin{bmatrix}0\\ 0\\ 60\end{bmatrix}u_\eta\\ \begin{bmatrix}a_n\\ q\end{bmatrix}=\begin{bmatrix}l_pM_\alpha-Z_\alpha & l_pM_q-Z_q & l_pM_\eta-Z_\eta\\ 0 & 1 & 0\end{bmatrix}\begin{bmatrix}\alpha\\ q\\ \eta\end{bmatrix}\end{gathered} \tag{5}$$

$$\begin{bmatrix}\dot{\beta}\\ \dot{r}\\ \dot{\zeta}\end{bmatrix}=\begin{bmatrix}Y_v & \frac{Y_r}{u_0}-1 & \frac{Y_\zeta}{u_0}\\ N_\beta & N_r & N_\zeta\\ 0 & 0 & -60\end{bmatrix}\begin{bmatrix}\beta\\ r\\ \zeta\end{bmatrix}+\begin{bmatrix}0\\ 0\\ 60\end{bmatrix}u_\zeta$$

$$\begin{bmatrix}a_y\\ r\end{bmatrix}=\begin{bmatrix}l_pN_\alpha+Z_\alpha & l_pN_q+Z_q & l_pN_\eta+Z_\eta\\ 0 & 1 & 0\end{bmatrix}\begin{bmatrix}\beta\\ r\\ \zeta\end{bmatrix} \quad (6)$$

Choice of Trim Conditions

In order to select the design points, the Mach number and altitude must be plotted with the flight time, or instead of them the dynamic pressure can be introduced with the change of flight time as shown in Fig. 3.

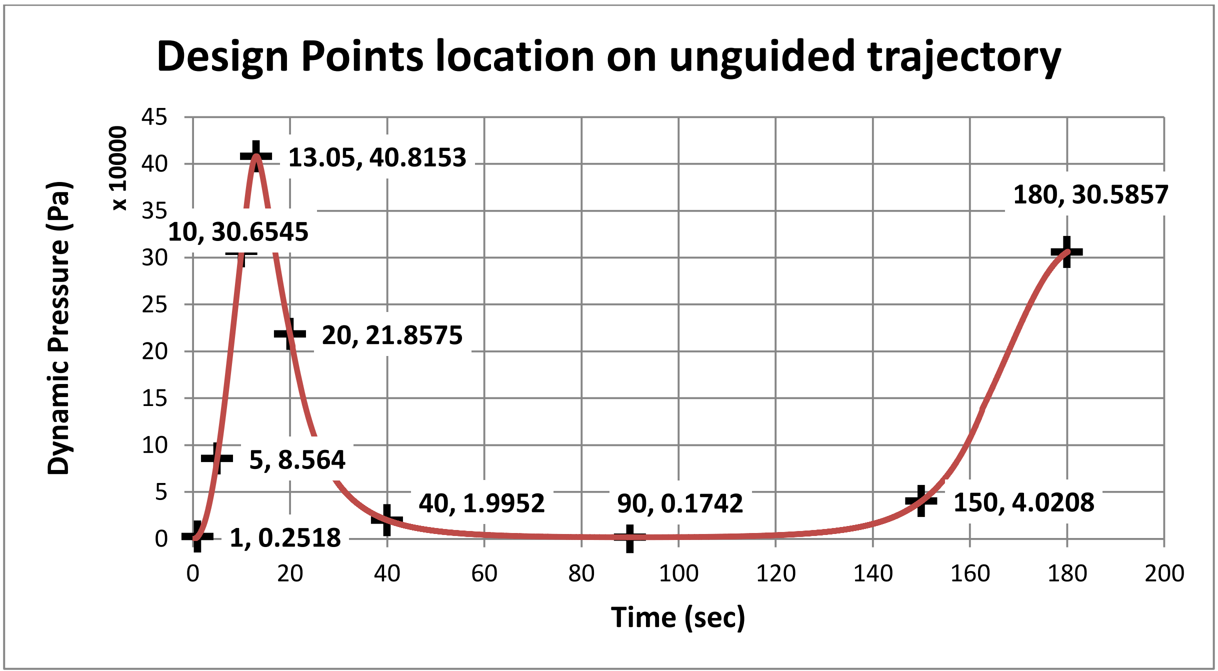

Fig. 3 Change of dynamic pressure during flight time

The design points must be at different dynamic pressure during the powered phase (which is from 0 to 13sec) and unpowered phase (from 13sec till flight end) in order to avoid repeating of design points or introducing large number of design points. Due to rapid change in dynamic pressure and missile states during the powered phase, a point is selected at every 5 sec. Due to moderate change in dynamic pressure and missile parameters during the unpowered phase, it is divided into regions with mid and final-points for each region are selected. Then the set of designing points are shown in Table 1 and Fig. 3.

Table 1. Set of designing points

point	1	2	3	4	5	6	7	8	9
Time [sec]	1	5	10	13	20	40	90	150	180

It is necessary to select a point at which the autopilot design is carried out and to generalize the structure of the controller for the other points. This point needed to be of higher dynamics point as presented in [4] that the higher dynamics model has achieved in alike manner or even better than gain scheduled classical control. From Fig. 3, it will be acceptable if choosing point at time (t=180sec) to be the nominal design point which has the state-space model:

$$\begin{bmatrix}\dot{\phi}\\ \dot{p}\\ \dot{\xi}\end{bmatrix}=\begin{bmatrix}0 & 1 & 0\\ 0 & -0.81 & -1928.84\\ 0 & 0 & -60\end{bmatrix}\begin{bmatrix}\phi\\ p\\ \xi\end{bmatrix}+\begin{bmatrix}0\\ 0\\ 60\end{bmatrix}u_{\xi}$$
$$\begin{bmatrix}\phi\\ p\end{bmatrix}=\begin{bmatrix}1 & 0 & 0\\ 0 & 1 & 0\end{bmatrix}\begin{bmatrix}\phi\\ p\\ \xi\end{bmatrix} \tag{7}$$

$$\begin{bmatrix}\dot{\alpha}\\ \dot{q}\\ \dot{\eta}\end{bmatrix}=\begin{bmatrix}-0.4628 & 0.9978 & -0.0036\\ -33.9164 & -0.7552 & -1.2481\\ 0 & 0 & -60\end{bmatrix}\begin{bmatrix}\alpha\\ q\\ \eta\end{bmatrix}+\begin{bmatrix}0\\ 0\\ 60\end{bmatrix}u_{\eta}$$
$$\begin{bmatrix}a_n\\ q\end{bmatrix}=\begin{bmatrix}26.2627 & -0.0029 & -0.0069\\ 0 & 1 & 0\end{bmatrix}\begin{bmatrix}\alpha\\ q\\ \eta\end{bmatrix} \tag{8}$$

$$\begin{bmatrix}\dot{\beta}\\ \dot{r}\\ \dot{\zeta}\end{bmatrix}=\begin{bmatrix}-0.4491 & 0.9978 & -0.0037\\ -33.1465 & -0.7442 & -1.289\\ 0 & 0 & -60\end{bmatrix}\begin{bmatrix}\beta\\ r\\ \zeta\end{bmatrix}+\begin{bmatrix}0\\ 0\\ 60\end{bmatrix}u_{\zeta}$$
$$\begin{bmatrix}a_y\\ r\end{bmatrix}=\begin{bmatrix}-25.4295 & 0.0028 & -0.0059\\ 0 & 1 & 0\end{bmatrix}\begin{bmatrix}\beta\\ r\\ \zeta\end{bmatrix} \tag{9}$$

Model Discretization

According to the Shannon sampling theorem [7], in order to select the suitable sampling time, it is necessary to realize the maximum natural frequency of the vehicle [7]. The maximum natural frequency appears in the pitch transfer function when the vehicle approaches target which is

Maximum natural frequency:

$\omega_n = 5.847$ [rad/s]

The sampling time will be:

$$T_s \le \frac{\pi}{\omega_n} = 0.5735\ [sec]$$
$$\xrightarrow{yields} T_s = 0.01\ [sec]$$

Although classical control needs nine design points to maintain its stability, it was found that MPC could maintain the same stability (or even better) with a single design point chosen at the highest dynamic pressure point (at t=180 sec) [4].

Discretization of the state-space model [7] of the highest dynamics point using sampling time (T_s = 0.01 sec) yields to:

$$\begin{bmatrix}\phi\\p\\\xi\end{bmatrix}(k+1)=\begin{bmatrix}0 & 0.00996 & -0.07951\\0 & 0.9919 & -14.44\\0 & 0 & 0.5488\end{bmatrix}\begin{bmatrix}\phi\\p\\\xi\end{bmatrix}(k)+\begin{bmatrix}-0.01668\\-4.77\\0.4512\end{bmatrix}u_{\xi}(k)$$
$$\begin{bmatrix}\phi\\p\end{bmatrix}(k)=\begin{bmatrix}1 & 0 & 0\\0 & 1 & 0\end{bmatrix}\begin{bmatrix}\phi\\p\\\xi\end{bmatrix}(k) \tag{10}$$

$$\begin{bmatrix}\alpha\\q\\\eta\end{bmatrix}(k+1)=\begin{bmatrix}0.9937 & 0.009912 & -7.805\times10^{-5}\\-0.3369 & 0.9908 & -0.009335\\0 & 0 & 0.5488\end{bmatrix}\begin{bmatrix}\alpha\\q\\\eta\end{bmatrix}(k)$$
$$+\begin{bmatrix}-1.961\times10^{-5}\\-0.003085\\0.4512\end{bmatrix}u_{\eta}(k) \tag{11}$$
$$\begin{bmatrix}a_n\\q\end{bmatrix}(k)=\begin{bmatrix}26.26 & -0.002858 & -0.006937\\0 & 1 & 0\end{bmatrix}\begin{bmatrix}\alpha\\q\\\eta\end{bmatrix}(k)$$

$$\begin{bmatrix}\beta\\r\\\zeta\end{bmatrix}(k+1)=\begin{bmatrix}0.9939 & 0.009914 & 8.075\times10^{-5}\\0.3293 & 0.9909 & -0.009642\\0 & 0 & 0.5488\end{bmatrix}\begin{bmatrix}\beta\\r\\\zeta\end{bmatrix}(k)$$
$$+\begin{bmatrix}-2.029\times10^{-5}\\-0.003187\\0.4512\end{bmatrix}u_{\zeta}(k) \tag{12}$$
$$\begin{bmatrix}a_y\\r\end{bmatrix}(k)=\begin{bmatrix}-25.4295 & -0.0028 & -0.0059\\0 & 1 & 0\end{bmatrix}\begin{bmatrix}\beta\\r\\\zeta\end{bmatrix}(k)$$

4. Predictive Control System Design

Roll Autopilot Design

The model predictive controller parameters are listed in Table 2.

Table 2. Roll MPC parameters

Horizon		Constraints			Simulation scenario	
N_u	N_2	Fin deflection	ϕ [°]	p [rad/sec]	ϕ	P
2	12	$-10 \le u_{\xi} \le 10$	$-45 \le \phi \le 45$	$-1.22 \le p \le 1.22$	step function	pulse function

All the unmeasured disturbances in the input and outputs are neglected. The two outputs are considered measured and fed-back to the controller. MPC minimizes an objective function that contains output tracking error and input control energy. For MIMO system relative weights could be assigned for input and outputs. Table 3 shows different controller time response for different input and outputs weights.

Table 3. Change of time characteristics with the weights

Case	Input weight		Output weight		t_r [sec]	t_s [sec]	M.O. %
	Weight	Rate	ϕ	p			
1	0	0.1	1	1	>10	>10	0
2	0.1	0.1	1	1	>10	>10	0
3	0	1	1	1	>10	>10	0
4	0	0.1	5	1	1.42	1.81	0
5	0	0.1	5	5	>10	>10	0
6	0	0.1	10	1	0.87	1	0
7	0	0.1	15	1	0.81	0.89	0
8	0	0.1	20	1	0.81	0.86	0

The response of normal acceleration at different weights is shown in Fig. 4. From this figure, one can choose the best results associated with the following weights (Table 4).

Table 4. Weights

Input weight		Output weight	
Weight	Rate	ϕ	p
0	0.1	15	1

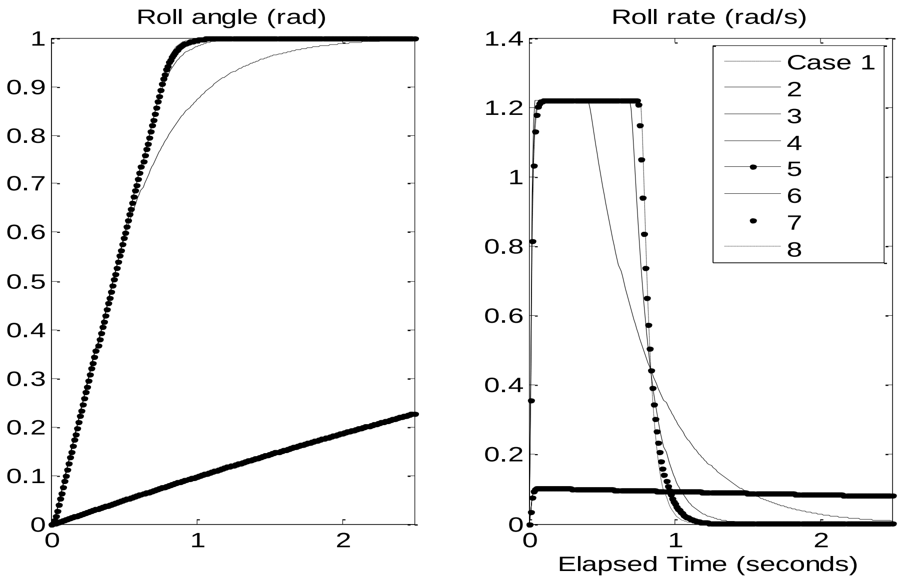

Fig. 4 Response of roll at selected weights

Normal Acceleration Autopilot Design

The model predictive controller parameters are listed in Table 5.

Table 5. Pitch MPC parameters

Horizon		Constraints			Simulation scenario	
N_u	N_2	Fin deflection	a_n [g]	q [rad/sec]	a_n	q
2	12	$-10 \leq u_\eta \leq 10$	$-10 \leq a_n \leq 10$	$-1.04 \leq q \leq 1.04$	step function	pulse function

All the unmeasured disturbances in the input and outputs are neglected. The two outputs are considered measured and fed-back to the controller. MPC minimizes an objective function that contains output tracking error and input control energy. For MIMO system relative weights could be assigned for input and outputs. Table 60 shows different controller time response for different input and outputs weights.

Table 6. Change of time characteristics with the weights

Case	Input weight		Output weight		t_r [sec]	t_s [sec]	M.O. %
	Weight	Rate	a_n	q			
1	0	0.1	1	1	0.53	1.6	3
2	0.1	0.1	1	1	> 20	> 20	0
3	0	1	1	1	0.64	> 20	11
4	0	0.1	5	1	0.36	3.04	6
5	0	0.1	1	5	> 20	> 20	0
6	0	0.1	5	5	0.53	1.47	4
7	0	0.1	0.1	0.1	0.64	> 20	11

The response of normal acceleration at different weights is shown in Fig. 5. From this figure, one can choose the best results associated with the following weights (Table 7).

Table 7. Weights

Input weight		Output weight	
Weight	Rate	a_n	q
0	0.1	1	1

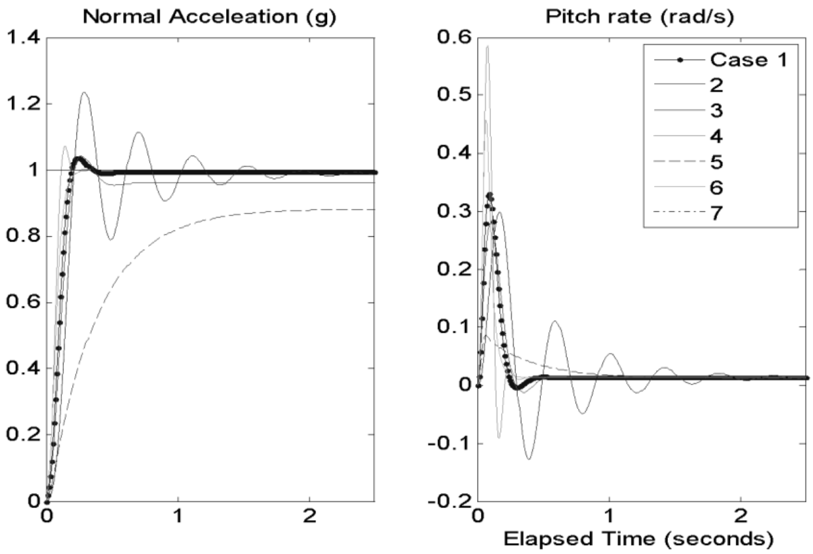

Fig. 5 Response of normal acceleration at selected weights

Lateral Acceleration Autopilot Design

The model predictive controller parameters are listed in Table 8.

Table 8. Yaw MPC parameters

Horizon		Constraints			Simulation scenario	
N_u	N_2	Fin deflection	a_y [g]	r [rad/sec]	a_y	r
2	12	$-10 \le u_\eta \le 10$	$-10 \le a_n \le 10$	$-1.04 \le q \le 1.04$	step function	pulse function

All the unmeasured disturbances in the input and outputs are neglected. The two outputs are considered measured and fed-back to the controller. MPC minimizes an objective function that contains output tracking error and input control energy. For MIMO system relative weights could be assigned for input and outputs. Table 9 shows different controller time response for different input and outputs weights.

Table 9. Change of time characteristics with the weights

Case	Input weight		Output weight		t_r [sec]	t_s [sec]	M.O. %
	Weight	Rate	a_y	r			
1	0	0.1	1	1	0.53	1.6	3
2	0.1	0.1	1	1	> 20	> 20	0
3	0	1	1	1	0.64	> 20	11
4	0	0.1	5	1	0.36	3.04	6
5	0	0.1	1	5	> 20	> 20	0
6	0	0.1	5	5	0.53	1.47	4
7	0	0.1	0.1	0.1	0.64	> 20	11

The response of lateral acceleration at different weights is shown in Fig. 5. From this figure, one can choose the best results associated with the following weights (Table 10).

Table 10. Weights

Input weight		Output weight	
Weight	Rate	a_y	r
0	0.1	1	1

5. Analysis of Autopilot Design

Figure 70 shows the block diagram of the simulation of autopilots with non-linear missile. Constructing the simulation as shown in [8] and performing it as presented in [9].

Cross wind is assumed to deviate the missile during its flight (Fig. 8a). Sensor noise is assumed to be a white noise with ±0.014 as shown in (Fig. 8b). Conducting the roll, pitch and yaw alone with the nonlinear model, the results are shown in Fig. 9, Fig. 10 and Fig. 11 respectively. These figures are represented only to clarify that each controller is robust along the whole flight trajectory even if conducted alone.

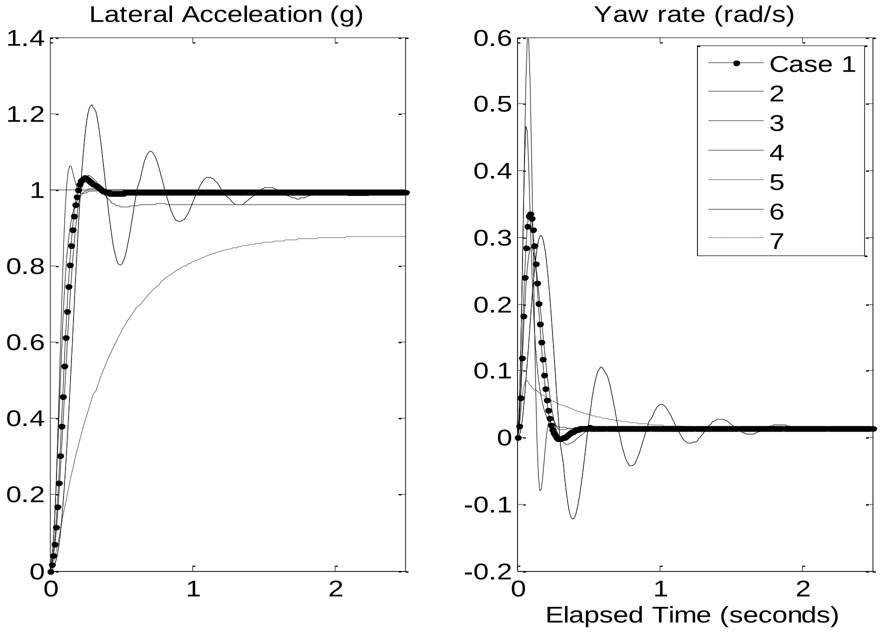

Fig. 6 Response of lateral acceleration at selected weights

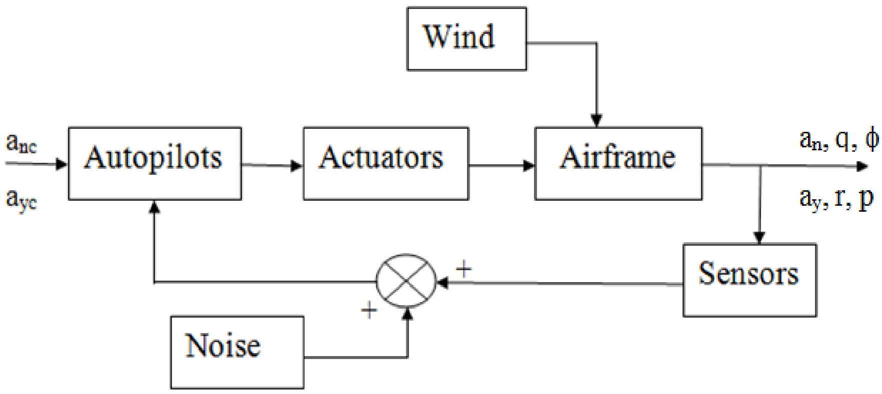

Fig. 7 Block diagram of the vehicle

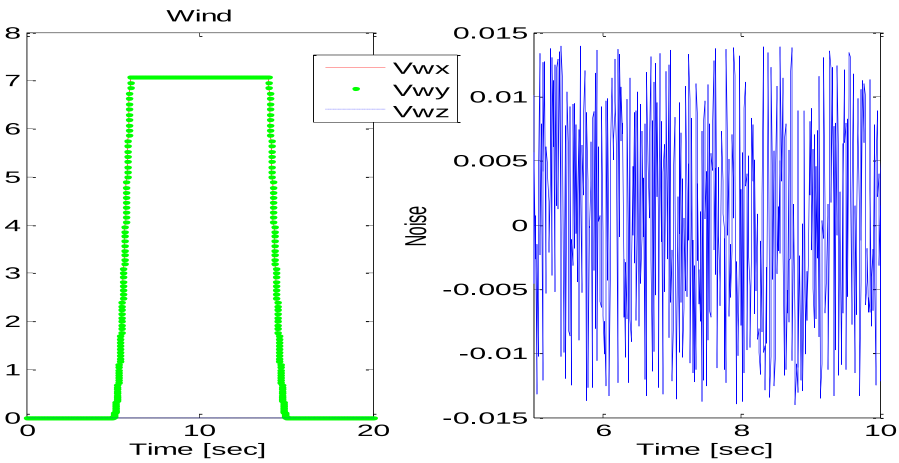

(a) (b)

Fig. 8 Wind and noise response

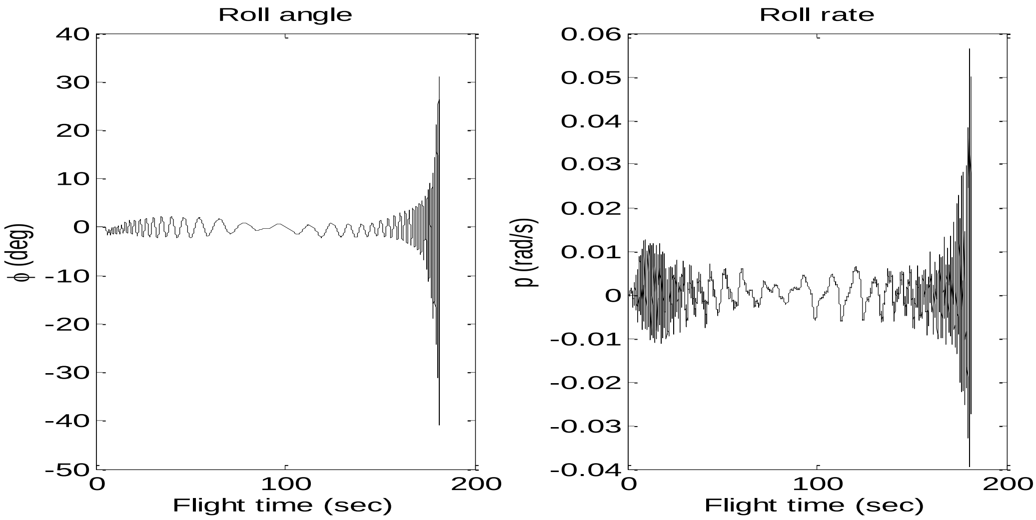

Fig. 9 Roll angle and roll rate responses for conducting roll autopilot alone

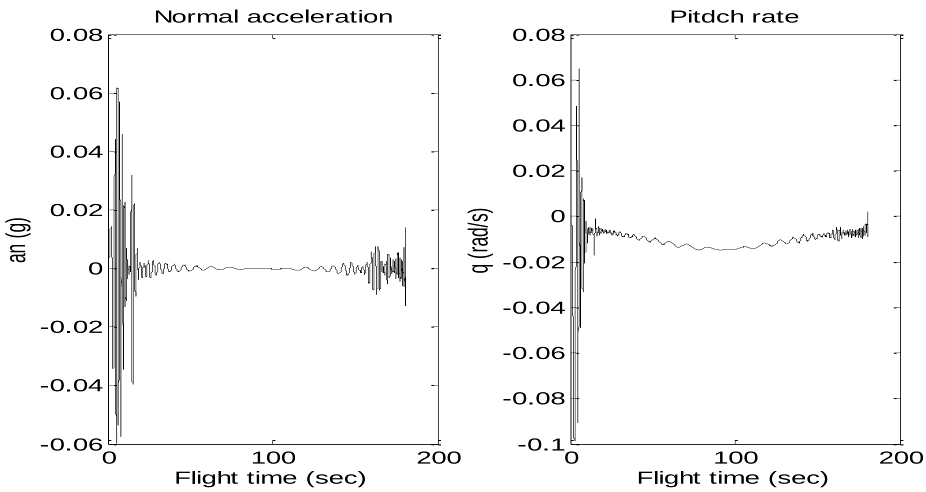

Fig. 10 Normal acceleration and pitch rate responses for conducting pitch autopilot alone

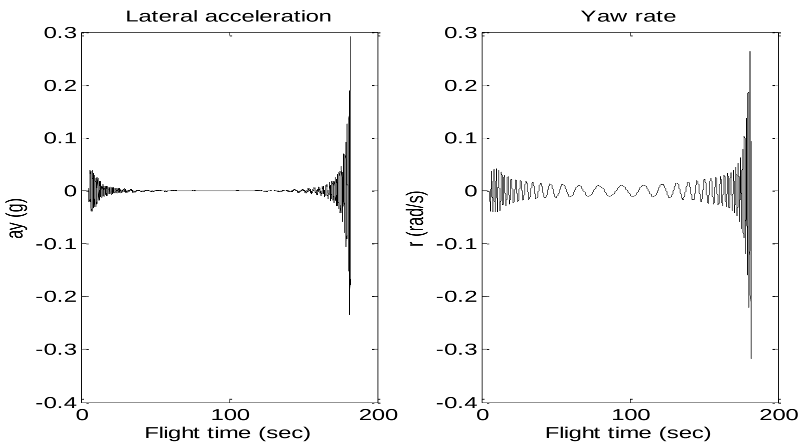

Fig. 11 Lateral acceleration and yaw rate responses for conducting yaw autopilot alone

When conducting the three autopilots with the nonlinear model and zero commanded normal and lateral accelerations, what are the improvements occurred to the missile flight rather than the guided missile affected by wind disturbance. These are shown in Fig. 12.

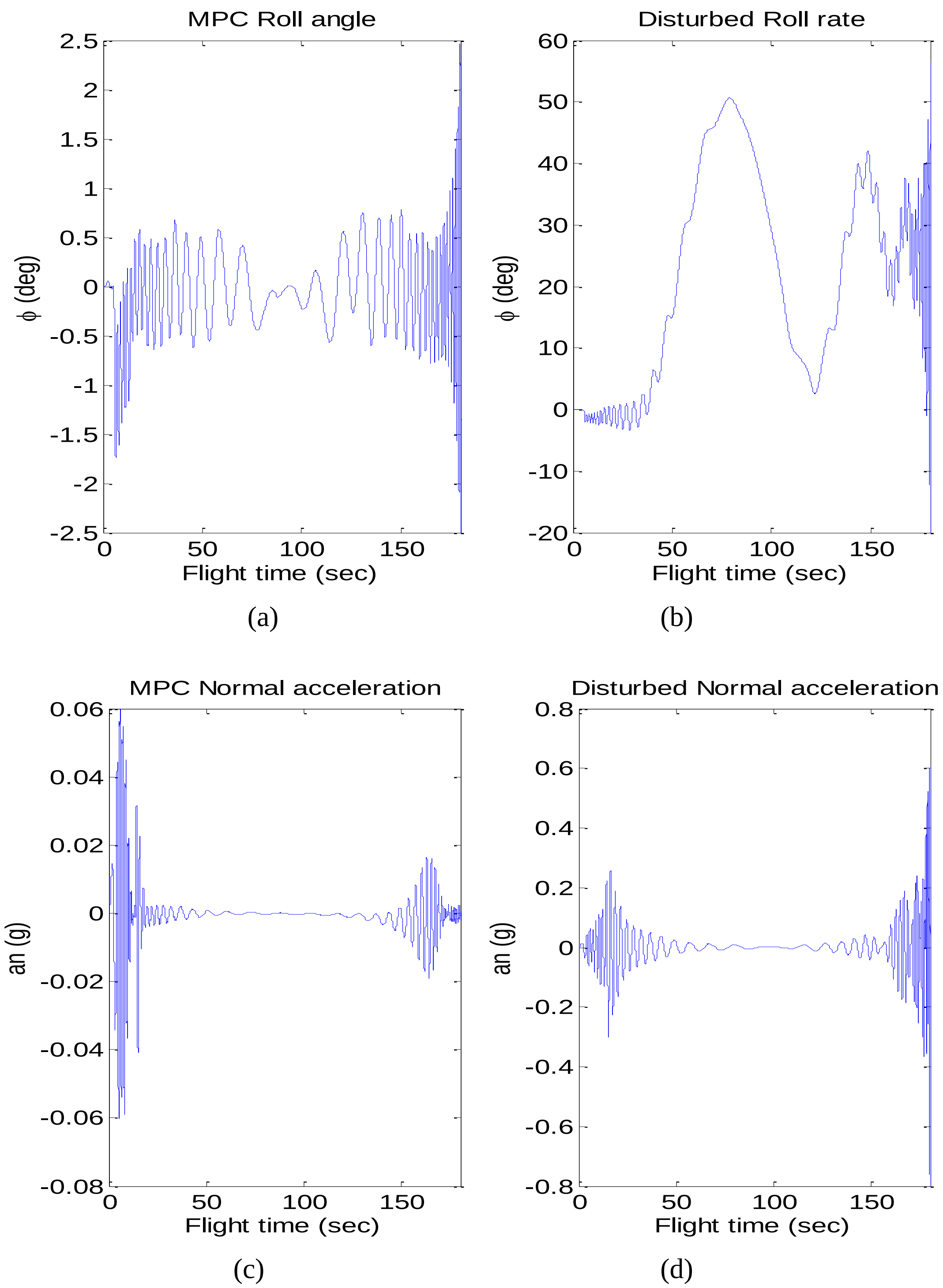

Fig. 12 Simulation results for predictive controlled and unguided missile

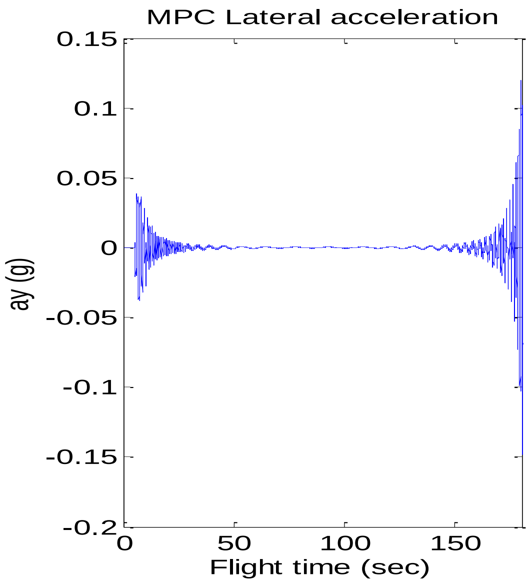

(e)

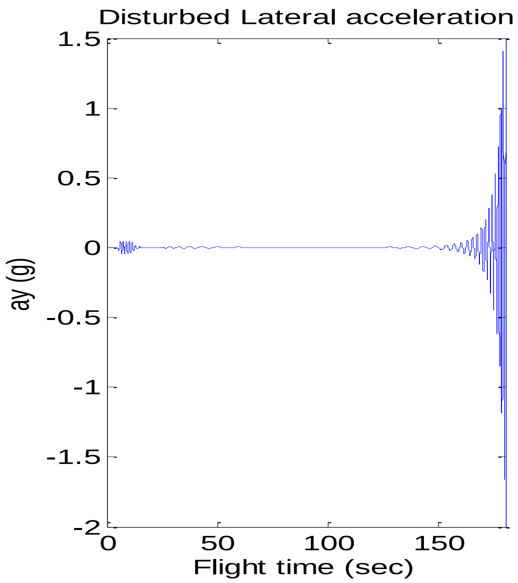

(f)

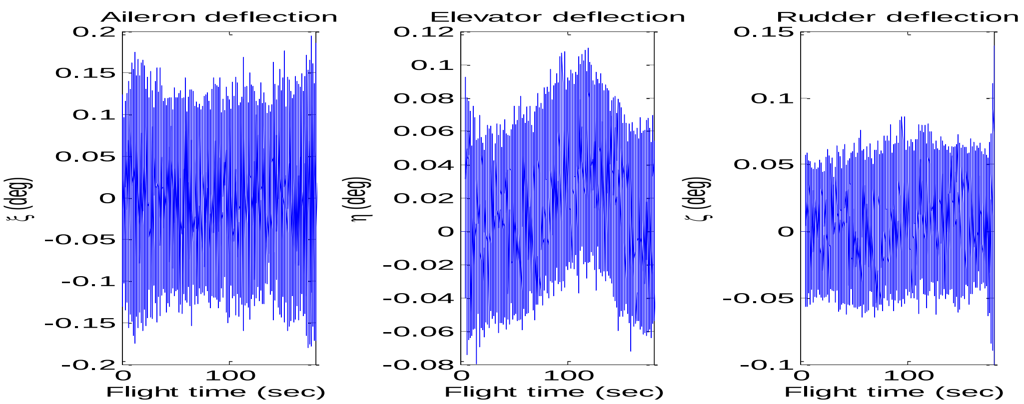

(g)

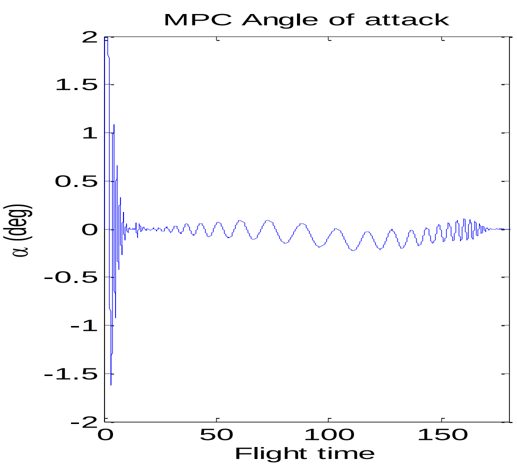

(h)

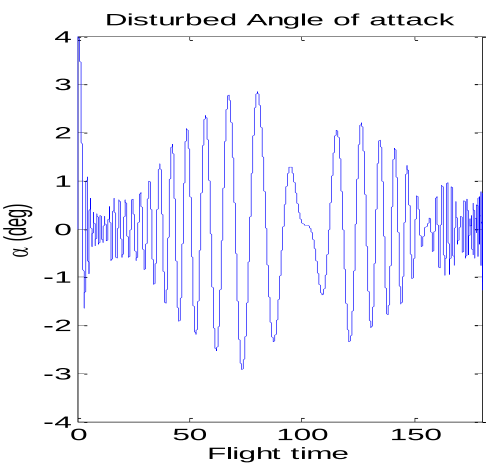

(i)

Fig.12 (Continued) Simulation results for predictive controlled and unguided missile

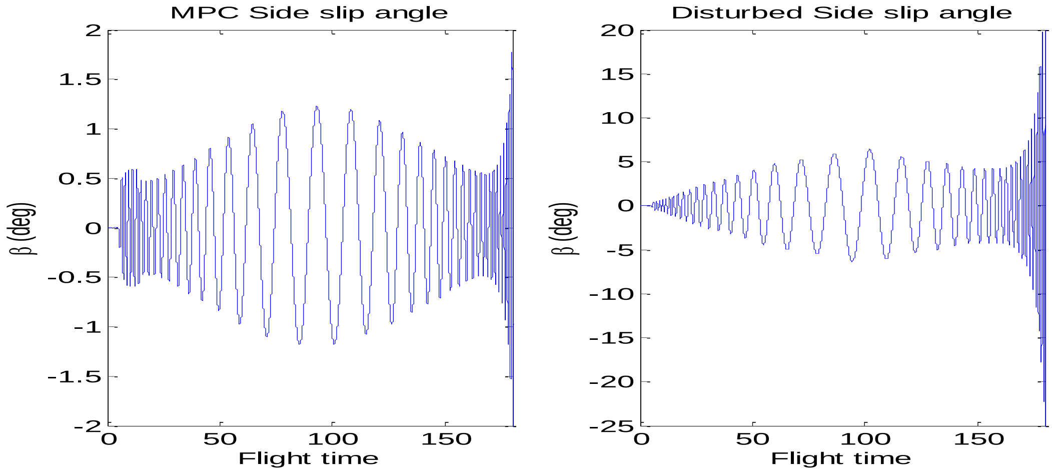

(j)

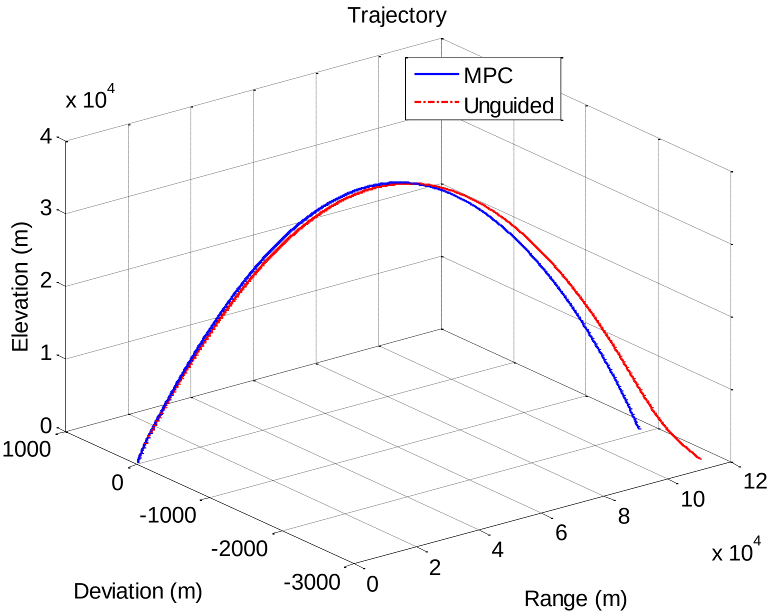

(k)

Fig. 12 (Continued) Simulation results for predictive controlled and unguided missile

MPC has improved the missile flight in the following aspects:
Conducting all autopilots, the responses of roll angle, normal and lateral accelerations characteristics are shown in Table 11.

Table 11. Closed loop statistical characteristics of MPC

Variable	Maximum	Minimum	Mean	Standard deviation	RMS
ϕ [°] - MPC	3.1445	-3.3653	-0.0648	0.4973	0.5014
ϕ [°] - Unguided	94.8405	-58.2746	21.2434	17.7061	27.6545
a_n [g] - MPC	0.0717	-0.0949	-0.0005	0.0144	0.0144
a_n [g] - Unguided	6.0693	-8.6251	-0.0002	0.2445	0.2445
a_y [g] - MPC	0.1654	-0.1821	0	0.0125	0.0125
a_y [g] - Unguided	3.711	-3.4793	0.0001	0.2436	0.2436

Figure 12a, c, e show that MPC has tracked the zero commanded roll angle, normal and lateral acceleration values with lower standard deviation.
0Figure 12i, j show that MPC has maintained the values of angle of attack and side slip angle and reduced their fluctuation.
Figure 12g shows that MPC maintained the value of aileron, elevator and rudder angles without violating the input signals constraints.
0Figure 12k shows that MPC decreased the value of side deviation as calculated in Table 12.

Trajectory characteristics are shown in Fig. 12k and Table 12.

Table 12. Trajectory characteristics of MPC and unguided missile

Controller	Time [sec]	Summit [km]	Range [km]	Side deviation [m]
MPC	183.47	36.842	116.29	2263.8
Unguided	182.26	36.876	115.42	2775.3

Remarks on the Results

Figure 12k shows that MPC and unguided trajectories are almost similar in values of the summit and range reached by the missile and this due to the approaching of normal and lateral acceleration means to zero where as the standard deviation caused the large fluctuation amplitude in the unguided missile responses.
The side deviation is existed due to absence of guidance as the autopilot damps the error of lateral acceleration not the side deviation.
At last MPC has verified its robustness and improved the performance of the unguided missile.

6. Conclusion

Normal acceleration, lateral acceleration and roll autopilots for a surface-to-surface missile have been designed using predictive control techniques. The lateral autopilot is designed to track the command signal of normal and lateral acceleration sent from guidance computer utilizing pitch and yaw rate and normal and lateral acceleration as feedback. The longitudinal autopilot is designed to eliminate rolling angle and damp any roll rate appears utilizing roll rate and roll angle as feedback. The choice of sampling time is based on the sampling theorem with utilizing maximum frequency appeared in the linearized model. Designing of MPC at specified point is robust at the higher dynamics model. The simulation of predictive controllers is created for each controller individually and all controllers activated. The simulation introduces wind model as a plant disturbance and noise added to the feedback to act as sensor noise. It is concluded that MPC is robust along the whole trajectory although it is of fixed algorithm.

7. References

[1] John H. Blacklock, “Automatic Control of Aircraft and Missile”, 2nd edition, John Wiley & Sons, Inc., (1991).
[2] Brian L. Stevens, Frank L. Lewis, “Aircraft Control and Simulation”, John Wiley & Sons, Inc., (1992).
[3] William B. Blake,” Missile DATCOM, User’s Manual -1997 FORTRAN 90 Revision”. AFRL-VA-WP-TR-1998-3009, Feb. (1998).

[4] M. S. Mohamed, A. M. Bayoumy, A. A. El-Ramlawy, G. A. El-Sheikh, " Comparison of Classical and Predictive Autopilot Design for Tactical Missile", ASAT - 15 – Military Technical College, Cairo, EGYPT, May 28 - 30, 2013.

[5] Farhan A. Faruqi , Thanh Lan Vu," Mathematical Models for a Missile Autopilot Design", Weapons Systems Division,Systems Sciences Laboratory,DSTO-TN-0449, (2002).

[6] Alberto Bemporad, Manfred Morari, N. Lawrence Ricker, "Model Predictive Control Toolbox, User's Guide", The MathWorks, Inc., 2012.

[7] Benjamin C. Kuo, "Digital Control Systems", 2nd ed., Saunders college publishing, (1992).

[8] Marc Rauw, "FDC 1.2 – A Simulink Toolbox for Flight Dynamics and Control Analysis", 2nd edition, May 2001.

[9] Peter H. Zipfel, "Modeling and Simulation of Aerospace Vehicle Dynamics", 2nd edition, AIAA, Inc., 2007.